International Journal of Nanomedicine

Dovepress
open access to scientific and medical research

Open Access Full Text Article

ORIGINAL RESEARCH

Mercaptopurine-Loaded Sandwiched Tri-Layered Composed of Electrospun Polycaprolactone/Poly (Methyl Methacrylate) Nanofibrous Scaffolds as Anticancer Carrier with Antimicrobial and Antibiotic Features: Sandwich Configuration Nanofibers, Release Study and in vitro Bioevaluation Tests

Samar A Salim,[1,2] Elbadawy A Kamoun,[1,3] Stephen Evans,[4] Shahira H EL-Moslamy,[5] Esmail M El-Fakharany,[6] Mohamed M Elmazar,[7] AF Abdel-Aziz,[2] RH Abou-Saleh,[8,9] Taher A Salaheldin[10]

[1]Nanotechnology Research Center (NTRC), The British University in Egypt (BUE), Cairo, 11837, Egypt; [2]Biochemistry Group, Chemistry Dep., Faculty of Science, Mansoura University, Mansoura, Egypt; [3]Polymeric Materials Research Dep., Advanced Technology and New Materials Research Institute (ATNMRI), City of Scientific Research and Technological Applications (SRTA-City), Alexandria, 21934, Egypt; [4]Molecular and Nanoscale Physics Group, School of Physics and Astronomy, University of Leeds, Leeds, LS2 9JT, UK; [5]Bioprocess Development Dep., GEBRI, City of Scientific Research and Technological Applications (SRTA-City), Alexandria, 21934, Egypt; [6]Protein Research Dep. GEBRI, City of Scientific Research and Technological Applications (SRTA-City), Alexandria, 21934, Egypt; [7]Faculty of Pharmacy, The British University in Egypt (BUE), Cairo, 11837, Egypt; [8]Biophysics Group, Dep. of Physics, Faculty of Science, Mansoura University, Mansoura, Egypt; [9]Nanoscience and Technology Program, Faculty of Advanced Basic Science, Galala University, Suez, Egypt; [10]Pharmaceutical Research Institute, Albany College of Pharmacy and Health Sciences, Albany, NY, 12144, USA

Correspondence: Elbadawy A Kamoun
Email e-b.kamoun@tu-bs.de; badawykamoun@yahoo.com

Background: 6-Mercaptopurine (6-MP) is a potential anti-cancer agent which its therapeutic and limitation applicability due to its high toxicity.

Objective: Herein, 6-MP was loaded into tri-layered sandwich nanofibrous scaffold (the top layer composed of poly methyl methacrylate/polycaprolactone (PMMA/PCL), the middle layer was PCL/PMMA/6-MP, and the bottom layer was PCL/PMMA to improve its bioactivity, adjusting the release-sustainability and reduce its toxicity.

Methods: Electrospun tri-layered nanofibers composed of PCL/PMMA were utilized as nano-mats for controlling sustained drug release. Four groups of sandwich scaffold configurations were investigated with alteration of (PMMA: PCL) composition.

Results: The sandwich scaffold composed of 2%PCL/4%PMMA/1%6-MP showed the best miscibility, good homogeneity and produced the smoothest nanofibers and low crystallinity. All fabricated 6-MP-loaded-PCL/PMMA scaffolds exhibited antimicrobial properties on the bacterial and fungal organisms, where the cytotoxicity evaluation proved the safety of scaffolds on normal cells, even at high concentration. Scaffolds provided a sustained-drug release profile that was strongly dependent on (PCL: PMMA). As (PCL: PMMA) decreased, the sustained 6-MP release from PCL/PMMA scaffolds increased. Results established that ~18% and 20% of 6-MP were released after 23h from (4%PCL/4%PMMA/1%6-MP) and (2%PCL/4%PMMA/1%6-MP), respectively, where this release was maintained for more than 20 days. The anti-cancer activity of all fabricated scaffolds was also investigated using different cancerous cell lines (e.g., *Caco-2, MDA*, and *HepG-2*) results showed that 6-MP-loaded-nanofibrous mats have an anti-cancer effect, with a high selective index for breast cancer. We observed that viability of a cancer cell was dropped to about 10%, using nanofibers containing 2% PCL/4%PMMA/1%6-MP.

Conclusion: Overall, the PCL: PMMA ratio and sandwich configuration imparts a tight control on long-term release profile and initial burst of 6-MP for anticancer treatment purposes.

Keywords: sandwich scaffold, PCL/PMMA, 6-MP, sustained drug release, anticancer, 6-Mercaptopurine, polycaprolactone/poly methyl methacrylate

Received: 9 August 2021
Accepted: 22 September 2021
Published: 11 October 2021

Introduction

Globally, cancer represents the second major cause of death, there were estimated to be 9.6 million deaths in 2018 according to studies carried by World Health Organization (WHO). Nearly, three quarters of deaths from cancer take place in middle- and low-income countries. Breast cancer is the most prolific cancer in women and represents about 25% of all female malignancies worldwide.[1] The most common treatment modalities of cancer are radiotherapy, chemotherapy and surgery but chemotherapeutic approaches are considered to be the main option for late stage and metastatic cancer treatment.[2] However, the traditional chemotherapeutic approaches are often inadequate due to features such as toxicity to the normal cells, poor drug uptake, difficulty targeting the delivery of drugs to tumor sites, insufficient therapeutic efficiency. Nanotechnology offers the potential to overcome some of these limitations and has been extensively studied in cancer diagnosis and treatment over the years. Nano-carriers such as nanofibers, liposomes, nanotubes, dendrimers, as well as nanoparticles are principally used for providing and preserving desired dose of therapeutic agents with slight toxicity.[3]

6-Mercaptopurine (6-MP) is a familiar commercial drug as anti-cancer, immune suppressant and anti-inflammatory properties.[4] It is also utilized as an effective treatment of inflammatory diseases (non-Hodgkin-lymphoma), immune diseases (rheumatologic disorders) and enhances avoidance of rejection following organ transplantation.[5] In the cell, 6-MP is metabolized by hypoxanthine phosphoribosyl transferase to methylated thioinosinic (the active form) to prevent synthesis of purine and is transformed later to thioguanine, which is a DNA inserting agent.[6] 6-MP goes through a complex biotransformation representing the drug inactive. Moreover, 6-MP suffers from limiting their bioavailability by increasingly prescribed to destroy by thiopurine S methyl transferase and Xanthine oxidase. Subsequently, this might lead to decrease its bioavailability approximately 16%.[7] Currently, the creation of nano-structured carrier materials in the form of nanofiber scaffolds have gained attention for a wide-range of applications. There are many advantages of nanofibers structure; such as control of release profile, high surface area, and enhance fiber strength. As result of these rich and valuable properties, nanofiber scaffolds could be used in numerous biomedical applications like, drug delivery systems,[8] tissue engineering[9] and wound dressings.[10] Electrospinning is considered one of the best options for producing nanofibers due to its flexibility, simplicity and cost-effectiveness, coupled with its capability to produce smooth as well as continuous nanofibers.[11]

There are several features the loaded nanofibers mats must display, such as hemo-compatibility, adequate tissue distribution, stability in biological fluids, control the size distribution, high drug loading efficiency, bioavailability, biodegradation and nontoxicity.[12] The structural, as well as physical, properties of polymers can be modified to specific requirements by blending between two or more polymers.[13] Mixing biopolymers physically, can result in the formation of novel properties which are superior to any one of the component of polymers used.[14] The miscibility between different biopolymers may create from several various interactions, such as hydrogen bonding, charge transfer for homo-polymer mixtures and dipole–dipole forces.[15] The thermoplastic polymethly methacrylate (PMMA) has been extensively used in medicinal applications and in optical systems (intraocular lenses).[16] Because of its stability in the oral environment, PMMA is widely utilized as a promising biomaterial in dentistry applications.[17] A semi-crystalline aliphatic polycaprolactone (PCL) is considered to be one of the most promising biodegradable and biocompatible aliphatic polymer; because of its biological and mechanical properties. It possesses a glass transition temperature around −60°C in addition to a melting point (MP) equal to 60°C.[18] Thus, PCL has been permitted by the US Food and Drug Administration (FDA) to utilize in medical applications and drug delivery systems.[19]

Numerous researchers have proved the advantages of coaxial/triaxial techniques for creation of nanofibrous mats for controlled release of drugs.[20,21] Even though such techniques produce efficient nanofibrous mats for sustained drug release, a complexity of creation process is the critical problem. Therefore, there is an essential to develop a simple technique with merits of controlling drug release. Sandwich-nanofibrous (tri-layered electrospun nanofibrous) model is a straightforward approach that can assist to release drugs in a very controlled manner. Previous studies have stated a sandwich-model of electrospun nanofibrous scaffold composed of PCL/shellac for releasing salicylic acid[19] and poly(lactic-co-glycolic acid)/collagen scaffold (PLGA/collagen) for releasing vancomycin, lidocaine and gentamicin[22] in a sustained fashion. Recently, Wang et al reported a design of tri-layered electrospun nanofibrous with controlled release of acyclovir.[23] While Kamath et al[24] used electrospinning technique to fabricate the sandwich models of IBU loaded PCL fibrous scaffolds which extensively observed for their efficacy in sustainable drug release. Recently, PCL/PMMA were prepared by different methods like casting method[18] and utilizing coaxial electrospinning technique,[25] where the whole results reported that homogeneity and

miscibility between the bi-polymers were developed in addition to improve optical, structural and electrical properties for drug delivery applications.

Here, we are exploring the first demonstration of loading 6-MP into sandwich electrospun PCL/PMMA nanofibrous scaffold as innovative anticancer platform, through electrospinning technique. The results present the physicochemical properties of different composite mats, their biocompatibility, anti-microbial activity, cytotoxicity, anti-cancer activity and their potential as a novel efficient sustained drug releasing biomaterial for cancer treatment.

Materials and Methods

Materials

Polymethyl methacrylate (PMMA, M_{wt} ~550 KDa) was purchased from Alfa Aesar, Germany. Polycaprolactone (PCL, M_{wt} ~ 14 KDa) was obtained from Sigma-Aldrich, Japan. Solvents of polymers, e.g., dimethylformamide (DMF purity ≥ 99%) and dichloromethane (DCM; purity ≥ 99%) were purchased from Fisher Scientific, UK and Sigma-Aldrich, France; respectively. 6-MP monohydrate (purity 98.5%) was obtained from Sigma-Aldrich, South Korea. Electrospinner model (MECC, NANON-01A, Japan) was utilized for nanofibers fabrication.

Fabrication of PCL/PMMA/6-MP Sandwich Nanofibrous Scaffolds

Briefly, 1% (v/v) of 6-MP loaded PCL/PMMA was prepared by adding 6-MP (10 mg/mL) in 4% (w/v) PMMA with different concentrations of PCL solution (0, 2, 4, 8%, w/v) which were dissolved in mixture of solvents (DMF: DCM) with ratio (2:1). Schematic explanation of layer-by-layer fabrication process is representing in Figure 1. 6-MP loaded PCL/PMMA sandwich nanofibrous scaffolds were created by spinning in sequence of bottom layer followed by 6-MP loaded as a middle layer and subsequently top layer as shown in Table 1. The solutions used to fabricate each layer were placed into 5 mL syringe connected with stain steal nozzle (22 G), then mounted into electrospinner system using tubeless spinneret supplied with high power supply up to 25 KV and operated at RH ~ 55% at room temperature.

Characterization of PCL/PMMA/6-MP Nanofiber Scaffolds

PCL/PMMA/6-MP nanofibers were instrumentally characterized by FTIR, SEM, XRD analyses and mechanical strength measurement (Supplementary Material).

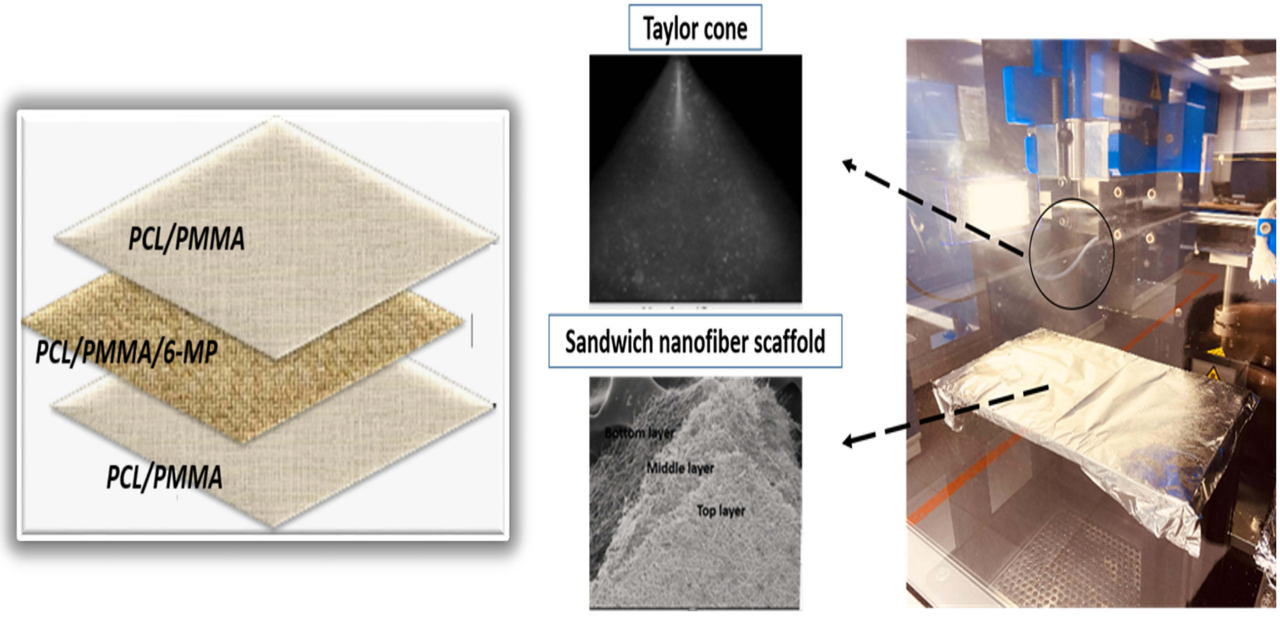

Figure 1 Schematic design of sequential electrospinning process of PCL/PMMA/6MP sandwich nanofibrous scaffold.

Table 1 Configuration of Sandwich and Non-Sandwich Electrospun PCL/PMMA/6-MP Nanofiber Scaffolds with Different Composition of Group Codes G1-G5

Group Codes	Bottom Layer (PCL/PMMA) (%, wt./v)	Middle Layer (PCL/PMMA/6-MP) (%, wt./v)	Top Layer (PCL/PMMA) (%, wt./v)
G1	2 mL, (8% PCL/ 4% PMMA) (2:1)	2 mL, (8% PCL/ 4% PMMA/ 1% 6-MP)	2 mL, (8% PCL/ 4% PMMA) (2:1)
G2	2 mL, (4% PCL/ 4% PMMA) (1:1)	2 mL, (4% PCL/ 4% PMMA/ 1% 6-MP)	2 mL, (4% PCL/ 4% PMMA) (1:1)
G3	2 mL, (2% PCL/ 4% PMMA) (1:2)	2 mL, (2% PCL/ 4% PMMA/ 1% 6-MP)	2 mL, (2% PCL/ 4% PMMA) (1:2)
G4	2 mL, (4% PMMA)	2 mL, (4% PMMA/ 1% 6-MP)	2 mL, (4% PMMA)
G5	Single layer, with 6 mL of (4% PMMA)		

Physicochemical Properties of PCL/PMMA/6-MP Nanofiber Scaffolds

Swelling Index (SI) and Hydrolytic Degradation of Nanofibrous Scaffolds

Dried scaffolds were weighed separately (W_d) before soaking in de-ionized water. After 10 min, swollen nanofibers were well dried by filter paper and the swollen nanofibrous mats were re-weighed (W_s), at interval times (0, 0.5, 1, 2, 3, 4, 5, 6 and 7 hour) to determine the weight change of sample against the time, as given in eq. (1).[26]

$$Swelling\ ratio(\%) = \frac{Ws - Wd}{Wd} X100. \quad (1)$$

To evaluate the relative amount of weight loss (%) due to the hydrolytic degradation from different nanofibrous scaffolds in an aqueous environment, each mat was sectioned in appropriate format and weighed. After that, each specimen immersed in 15 mL of de-ionized water and saved in an incubator at room temperature for varied time intervals: (1, 3, 6, 8, 12, 16, 20 and 28 day). Subsequently, each piece was eliminating from the medium, dried in a vacuum oven and weighed (*Wf*). The weight loss (%) was calculated using eq. (2). Where, Wi is the original weight of the mat sample.

$$Weight\ loss(\%) = \frac{Wi - Wf}{Wi} X100. \quad (2)$$

In vitro Bio-Evaluation Tests

Evaluation of Antimicrobial Activity in vitro of Nanofibrous Scaffolds

To describe the resistance of tested human pathogens, antimicrobial susceptibility tests were investigated using different antibiotics categories such as; *Kanamycin* (30 mcg), *Ampicillin* (10 mcg), and *Cephaloridine* (30 µg) for *Klebsiella rhinoscleromatis, Streptococci sp., Shigella sp*., and *Staphylococcus epidermidis* besides *Itraconazole* (10 µg), *Fluconazole* (25 mcg), and *Clotrimazole* (10 mcg) for *Candida tropicalis*, and *Candida krusei* via disc diffusion method.[27,28] Subsequently, antimicrobial activities of tested composite mats that contains different concentration of PCL as follows: (8% PCL/4% PMMA/1% 6-MP) (A), (4% PCL/ 4% PMMA/1% 6-MP) (B), and (2% PCL/4% PMMA/1% 6-MP) (C) were evaluated statistically and compared with (4% PMMA/1% 6-MP) (D), (4% PMMA) (E), and (1% 6-MP) (F) utilizing agar-well diffusion assay.[29]

An agar-well diffusion assay was used to calculate the antagonistic activity of different composed mats as liquid phase against six of multi drug-resistance human pathogens. Briefly, *Mueller Hinton* agar medium that used for fungal cells was prepared by dissolving 17.5 of acid Hydrolysate of casein, 2.0 g of beef extract, and 1.5 g of starch, using 1L distilled water and the pH was adjusted at 7.3, then 15 g of agar was added. For bacterial cells, nutrient agar medium was prepared (g/L) using 5 g peptone, 1.5 g yeast extract, 1.5 g beef extract, and 5 g NaCl that solidified using 15 g agar. Via spread plate method, these solidified plates were swabbed with tested human pathogens separately. Then, wells were bored using different metal cork borers (2, and 6 mm) and 50 µL of different tested composites were loaded and placed at 4°C for 8 h. These plates were incubated at 30°C for fungal cells and at 37°C for bacterial cell for 48 h. At that time, the resultant clearing (inhibition) zones were noted and the average of three zones diameters was calculated for each composite.

Hemocompatibility of PCL/PMMA/6-MP Nanofibrous Scaffolds

The important tool to observe the biocompatibility of examined nanofibers is testing the capability of a scaffold to enhance the human RBCs discharging their hemoglobin

content. Briefly, a sample of healthy blood was collected and mixed with EDTA solution to evade its clotting. 700 µL was a total volume of Ca^{+2}-Mg^{+2} free DPBS buffer were lightly mixed with 10 µL of the obtained blood. 100 mg of samples (G1, G2, G3, G4 and G5) were added individually to diluted blood in each tube. Furthermore, 100 µL of DMSO (0.5%) and Triton X-100 were replacing the samples in the negative and positive controls, respectively. Both of control tubes and tested tubes were incubated for 3.5 h at 37°C followed by 30 min interval inverting. Subsequently, all tubes were centrifuged for 15 min at 10,000 rpm. The mixture (1:1) of cyanmethemoglobin reagent and each sample was prepared and the absorbance was observed spectrophotometric at 540 nm using nanofibers without blood and Ca^{+2}-Mg^{+2} free DPBS buffer as blank.[30]

Assay of Drug Content and Drug Loading Efficiency into Nanofibrous Scaffolds

A spectrophotometric method was used to determine the active drug content on a representative scaffold. To calculate the amount of drug entrapped from each mat, fibrous mat discs (1 × 1 cm) were dissolved in known volume of DMF and DCM and absorbance was recorded at the absorption maxima of 340 nm for 6-MP by using UV-spectrophotometer (Agilent Cary 5000 UV-Vis-NIR spectrophotometer). The different discs of mats were tested randomly from different positions on the fibrous scaffolds. Consequently, the different concentration was obtained from standard calibration curve of 6-MP dissolved in DMF and DCM. The amount of active drug and the efficiency of drug loading is defined as percent of labeled drug content to the weight of the sample and as percent of calculated drug to the initial drug added according to eqs. 3, 4, and 5, respectively.

$$Amount\ of\ drug = drug\ Conc\ x\ volume \tag{3}$$

$$Drug\ content = \frac{Amount\ of\ drug}{amount\ of\ fiber} X100. \tag{4}$$

$$Drug\ loading\ efficiency = \frac{amount\ of\ drug}{intial\ amount\ of\ drug} X100. \tag{5}$$

Drug Release Profile and Kinetics Study

6-MP release profile was carried out for 21 days by suspending discs of different mats in 50 mL of phosphate buffered saline (DPBS, pH 7.4). At exact interval times, 1 mL of sample was drawn from the stock vial and placed in a clean quartz cuvette to read at 340 nm then the 1 mL returned back to the sample stock to keep the dilution factor fixed. The concentration of drug released was found from standard calibration curve of 6-MP, where the cumulative drug release was determined.

Cytotoxicity of PCL/PMMA/6-MP Nanofibrous Scaffolds

Effectiveness of nanofibers samples on cell viability of *HFB-4 cells* (normal human melanocytes) was examined using cell viability assay (MTT) as previously mentioned by Mosdam[31] and Almahdy et al.[32] Briefly, *HFB-4* (1.0×10^3) cells were triplicate seeded in 96-well sterile flat bottom tissue culture micro-plates and cultured in DMEM media (Lonza, USA) supplemented with 10% fetal bovine serum (FBS), subsequently cells were incubated at 37°C in 5% CO_2 incubator for 24 h. Then, nanofiber discs at concentrations of (0.125, 0.25, 0.5, 1, and 2 mg/mL) were added to cells in triplicates and incubated at 37°C in 5% CO_2 incubator. After 48 h of incubation, nanofiber discs were discarded, then the cells were washed with 1.0 M PBS three times to eliminate dead cells and debris. Subsequently, 200 µL of (0.5 mg/mL) MTT solution was added to each well and incubated for about 2–3 h and 5% CO_2 at 37°C. The formazan crystals were solved in 200 µL/well of DMSO and the absorbance was recorded using micro-plate ELISA reader at 595 nm. The cell viability was calculated by comparing to control wells having cells only without nanofiber discs using the following formula: (A) test / (A) control × 100%. Where, IC_{50} values were estimated using the *GraphPad Instat 6.0* software. All experiments were measured three times and untreated control cells were acted as a negative reference.

Anticancer Activity of PCL/PMMA/6-MP Nanofibrous Scaffolds

Antitumor activity of tested nanofibers samples was investigated in vitro through examined their cytotoxicity effect by using MTT assay on the different tumor cell lines, as revealed aforementioned. Human cancer (*Caco-2, HepG-2*, and *MDA*) cells (all cell lines were obtained commercially from GEBRI, SRTA-City, Egypt) were seeded at concentrations of 1.0×10^4 / well in 96-well flat bottom plates for overnight in 5% CO_2 atmosphere. After cell attachment, tested discs at different concentrations (0.125, 0.25, 0.5, 1 and 2 mg/mL) were implanted to each well. All plates were incubated for 48 h in 5% CO_2 incubator. Subsequently, cells were washed with fresh medium three times to get rid of dead cells, debris and 200 µL of MTT (0.5 mg/mL) solution in PBS buffer, were

added to each well then incubated for 2–3 h in 5% CO_2 incubator to allow viable cells metabolize MTT. Then, IC_{50} values and cell viability were recorded as revealed above in addition to the selectivity index (SI) for each sample were calculated by dividing the mean value of IC_{50} of *HFB-4* cells by the mean value of IC_{50} of tumor cells.

Results and Discussion

Optimization of Spinning Conditions

Numerous spinning conditions are required to achieve accepted morphological nanofibers in terms of smooth, beads less, nanofiber production.[33] PCL and PMMA were blended in different ratios then fabricated under different voltage, and adapted solution feed rate, as explained in Table 2. Table 2 exhibits the spinning conditions optimization for preparation of nanofibrous scaffolds with different compositions. The distance between syringe-nozzle and the plate collector coated with aluminum foil was kept constant at 15 cm. It was noticed that, the applied voltage and feed rate of polymer solution represented one of the critical parameters to control the topography of nanofibers fabrication. It was established that, the solutions that have ratio of PMMA ≥ PCL (G2, G3, G4 and G5) were affected by high voltage (22–23 KV) and feed rate around (0.7–1.0mL/h) resulted in uniform nanofibrous mats. Meanwhile, the scaffold composed of the highest ratio of PCL (G1) was fabricated using an applied voltage up to 16 KV and feed rate ~1.4mL/h. All nanofibrous scaffolds were created in the form of sandwich nanofibrous mats by spinning layer-by-layer sequence. The top and bottom layers of all scaffolds were of the same composition; whilst the middle layer was loaded with 6-MP, as represented below in Table 1. The collected sandwich nanofiber mats were dried using vacuum oven for 24 h to remove residual solvents and then were stored in dried, cold, conditions to avoid any possible contamination.

Characterization of PCL/PMMA/6-MP Nanofiber Scaffolds

FTIR Analysis

FTIR spectra were used to assess the incorporation of 6-MP physically into PMMA/PCL blend nanofibrous scaffold. Figure 2 represents the FTIR absorption spectra of different nanofibers composed of various concentration of PCL (i.e., 0, 2, 4 and 8%, w/v) blended into 4% PMMA, in addition to loaded 6-MP. PMMA displayed characteristic absorption peaks at ν 1725 and 1140 cm^{-1} which are assigned to C=O and O-CH_3 respectively as clearly showed in Figure 2B. Specific absorption bands of PCL were detected at ν 1728, 1468, 1171 cm^{-1} which were related to C=O, CH_2 bending and C-O-C modes respectively, as shown in Figure 2C. The characteristic absorption bands of both PCL and PMMA were represented in all scaffolds composed of PCL and PMMA in addition to 6-MP, as shown in Figure 2D–F. Some bands changed and shifted their intensity, others disappear, and a new absorption band appeared nearly at ν1200 cm^{-1} which this is a significant indication for compatibility between PMMA and PCL; this result is in agreement with previous observations by Abdelrazek et al.[18] While, the characteristic absorption peaks of 6-MP are due to C—N stretching and S—H bending at (ν 1450 and 768 cm^{-1}, respectively) was clearly observed in Figure 2A of the pure drug (6-MP). 6-MP loaded-scaffolds were obviously showed specific absorption band around at ν 1450 cm^{-1} which is assigned to the C—N group. This observation proved that the spectrum of PCL/PMMA/6-MP realized all characteristic spectrum absorption bands of all scaffold compositions.

Table 2 Optimization of Spinning Conditions of Fabrication of Electrospun PCL/PMMA/6-MP Nanofiber Mats with Different Composition in Codes G1, G2, G3, G4 and G5

Group	PCL/ PMMA Ratio	PCL Concentration (%, w/v)	PMMA Concentration (%, w/v)	6-MP Concentration (%, w/v)	Voltage (KV)	Feed Rate (mL/h)	Distance Between Tip and Collector (cm)
G1	2:1	8%	4%	1%	16	1.4	15
G2	1:1	4%	4%	1%	22	1	15
G3	1:2	2%	4%	1%	23	0.7	15
G4	-	-	4%	1%	23	0.7	15
G5	-	-	4%	-	23	1	15

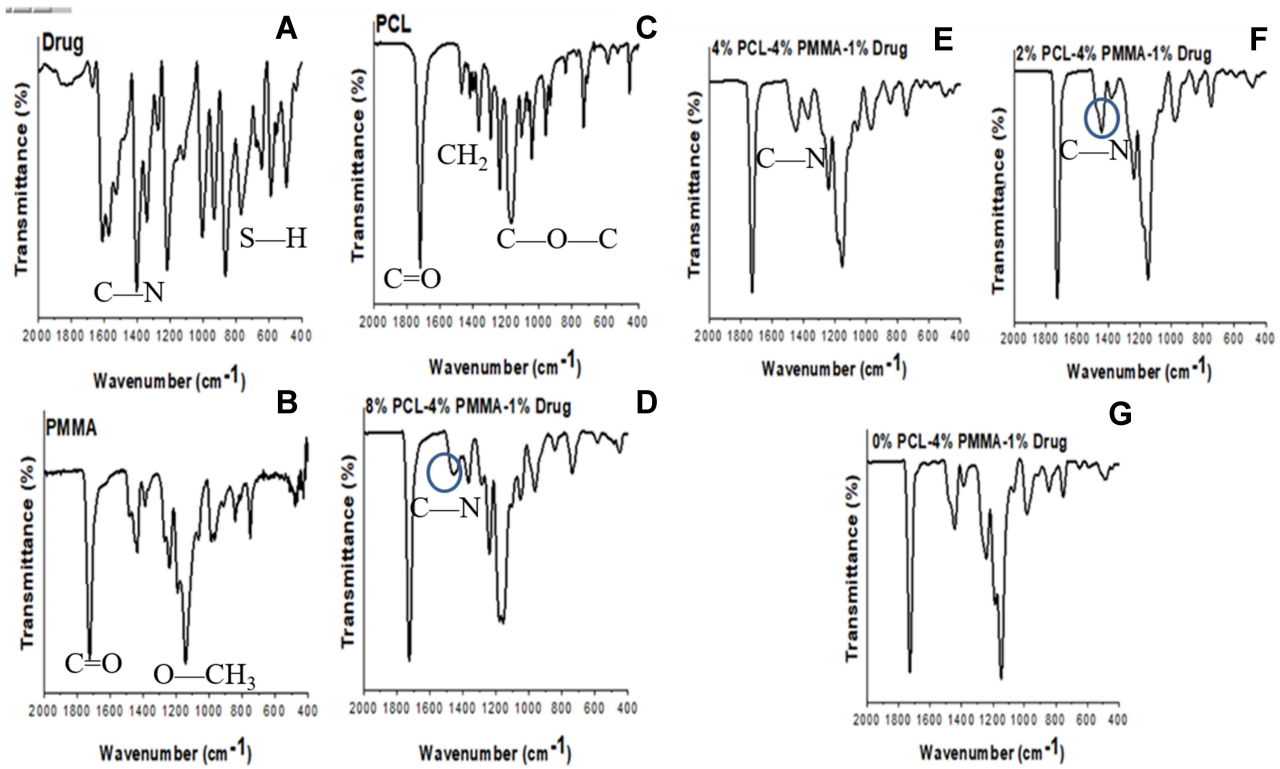

Figure 2 FTIR spectra of (**A**) 6-MP, (**B**) PMMA, (**C**) PCL, (**D**) 8% PCL/4% PMMA/1% 6-MP, (**E**) 4% PCL/4% PMMA/1% 6-MP, (**F**) 2% PCL/4% PMMA/1% 6-MP and (**G**) 4% PMMA/1% 6-MP.

Morphology Investigation of Sandwich Nanofibrous Scaffolds

The sandwich configuration structure and topography features of tri-layered nanofibrous scaffolds were investigated by SEM as shown in Figures 3 and 4. Figure 3 represents the tri-layered configuration (sandwich structure) of different compositions of nanofibers at different magnifications. The cross-sectional images of the scaffolds obviously show empty spaces between the layers whenever the concentration of PCL decrease. While, interspace of scaffolds can be explained as the relative evaporation rate of DMF (solvent of PMMA), less than DCM (solvent of PCL); so the nanofibers were created with high concentration of PCL are tightly bound together in contrast of scaffolds have low concentration of PCL (Figure 3). The sandwich configuration of all 6-MP-loaded scaffolds with different ratios of PMMA: PCL were successfully fabricated using electrospinning technique. The diameters of fibers prepared by electrospinning technique depend on the nature of polymer and the conditions of process.[34] In this study, PCL was added to PMMA with different ratios (0, 2, 4 and 8% w/v) to obtain uniform and beadles 6-MP-loaded nanofibrous mats (Figure 3).

As represented in Figure 4, the diameter of electrospun NF was decreased significantly by decreasing PCL concentrations. The average diameter of different scaffolds was calculated using image J software by detecting and analyzing of random fifty nanofibers. The average diameter of NFs ranged between ~ 0.8, 0.5 and 0.4 μm for (PCL: PMMA) (2:1, 1:1 and 1:2) respectively; while the diameter of nanofibers remains almost without change up to 0.2 μm for 6-MP-loaded and unloaded onto PMMA nanofibrous mats. The nanofibers were arranged randomly with uniform and smooth feature and their pores increased with increasing concentration of PMMA in mats.[34] However, the pores of mats decreased notably with increasing the concentration of PCL in composite nanofibrous mats.

XRD Analysis

The crystallographic structure of electrospun nanofibrous mats was obtained by XRD patterns as shown in Figure 5. XRD patterns show drug induced changes in the crystallinity of nanofibers. The X-ray diffraction scan of pure 6-MP showed the fingerprints with sharp observed patterns,[2] indicating its crystalline structure which indicated at 2θ 15.5°, 14.8°, 23.9°, 27.6° and 30°. XRD patterns of PMMA/PCL

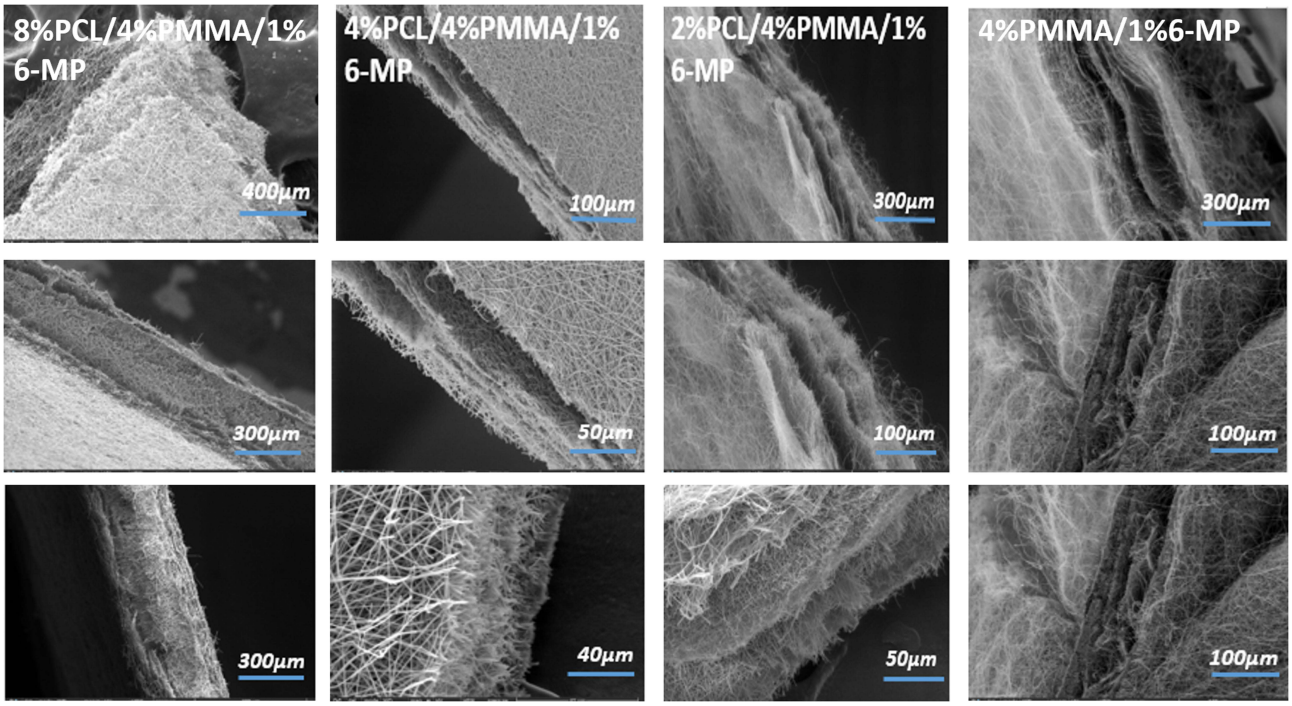

Figure 3 SEM images of the sandwich configuration at different image magnification.

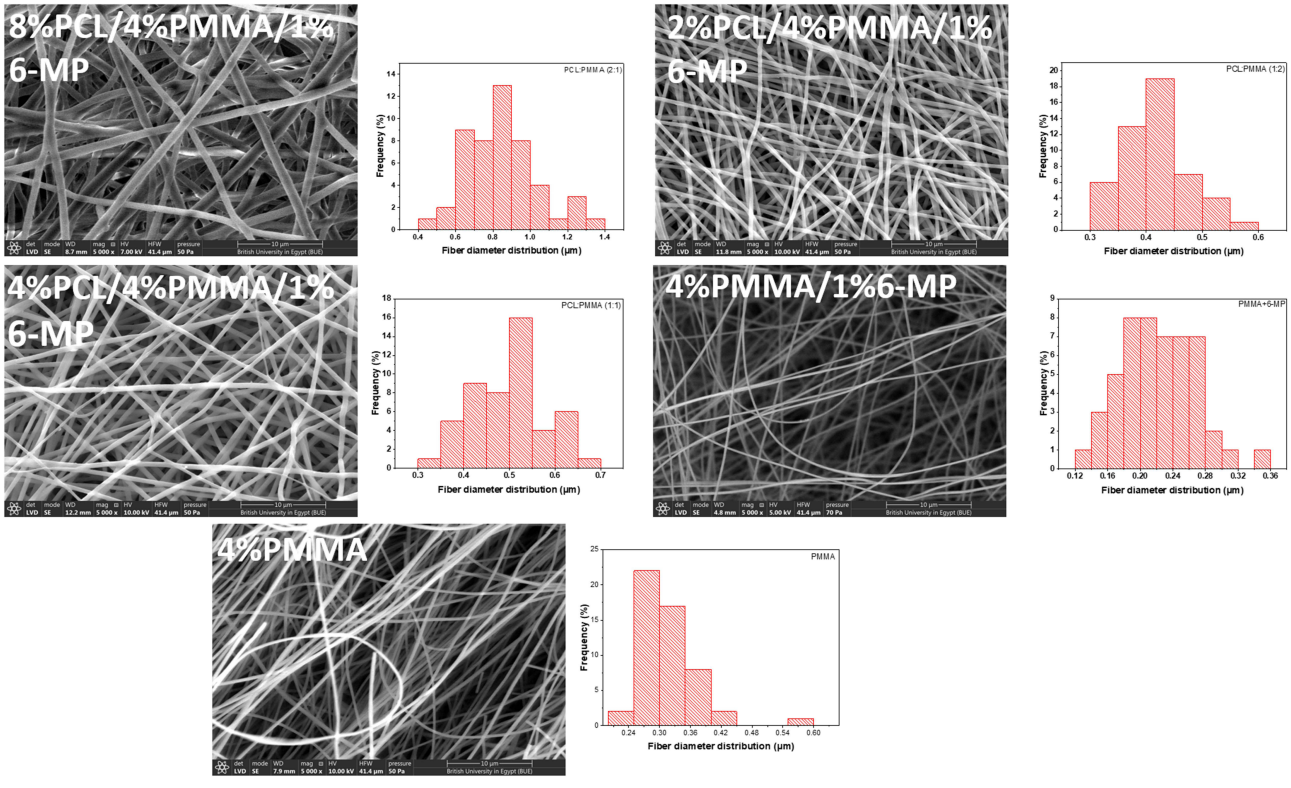

Figure 4 Surface morphology of fabricated nanofibrous scaffolds of (8% PCL/ 4% PMMA/ 1% 6-MP), (4% PCL/ 4% PMMA/ 1% 6-MP), (2% PCL/ 4% PMMA/ 1% 6-MP), (4% PMMA/ 1% 6-MP) and 4% PMMA with original magnification ×5000.

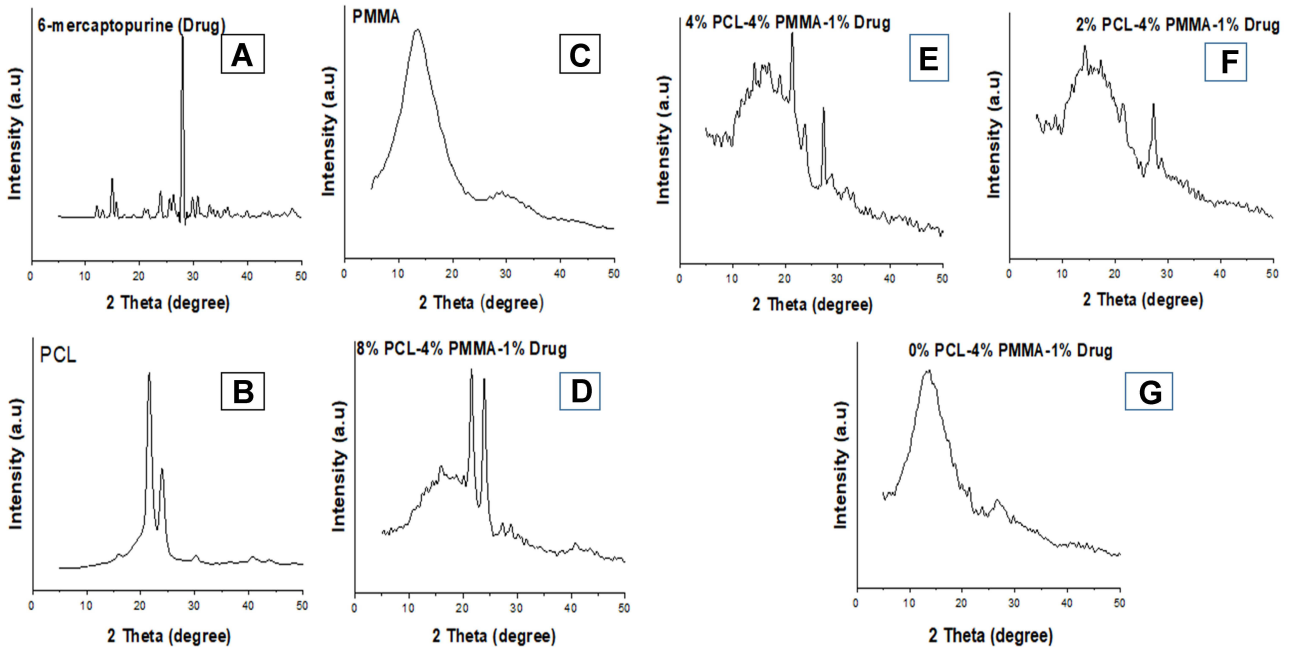

Figure 5 X-ray diffraction patterns of (**A**) pure 6-MP, (**B**) PCL, (**C**) PMMA, (**D**) (8% PCL/4% PMMA/1% 6-MP), (**E**) (4% PCL/4% PMMA/1% 6-MP), (**F**) (2% PCL/4% PMMA/1% 6-MP) and (**G**) (4% PMMA/1% 6-MP).

nanofibers reveal two broad patterns at 2θ 13° and 29° for PMMA and clear intense patterns at 2θ 21.6° and 24° of PCL which indexed to amorphous and orthorhombic crystalline structure, respectively.[18] Moreover, XRD patterns of PCL/PMMA blend mats showed reduced crystallinity of both drug and PCL which was the critical indication of miscibility between polymers[18] and 6-MP. Previously, the degree of crystallinity is affected by the evaporation rate of used solvent.[35] The crystallinity of different 6-MP-loaded mats was calculated from XRD pattern using Origin pro software, the results noticed that 6-MP and PCL have a high degree of crystallinity about 62% and 47%, respectively; while the 6-MP-loaded nanofibers represented low crystallinity about 24, 16, 15 and 48% for (8% PCL/4% PMMA/1% 6-MP), (4% PCL/4% PMMA/ 1%6-MP) (2% PCL/4% PMMA/1% 6-MP) and (4% PMMA/1% 6-MP), respectively. This implies that the crystallinity of 6-MP-loaded PMMA/PCL increased with increasing PCL content in mats. These results are consistent with results obtained by Elashmawi et al, who found that the addition of PMMA to PVDF reduce the crystallinity structure and completely miscible among two polymers.[36]

Mechanical Stability of PCL/PMMA/6-MP Nanofiber Scaffolds

Young's modulus, elongation-at-break (%) and maximum strength of composite nanofibers were measured to study the mechanical stability under mechanical loads with different PCL contents in scaffolds (8%PCL/4%PMMA/1% 6-MP), (4%PCL/4%PMMA/1%6-MP), (2%PCL/4% PMMA /1%6-MP), (4%PMMA/1%6-MP) and (4% PMMA), as displayed in Figure 6A and B. Interestingly, the incorporation of low concentration of PCL (2, 4%, w/v) into PMMA nanofibers significantly enhanced the mechanical strength, compared to nanofibers with high concentration of PCL (8%) and scaffolds without PCL. These results reveal that, the compatibility between PMMA with low concentration of PCL might realize as result of blending mechanism of 6-MP. Meanwhile, the incorporation of 1% 6-MP to sandwich form of PCL and PMMA solution could generate porous interconnected scaffold, that enhances mechanical stability of nanofibrous mats and in turns facilitates cell proliferation, adhesion and differentiation.

Swelling Study and Hydrolytic Degradation of PCL/PMMA/6-MP Nanofibrous Scaffolds

Drug-loaded NFs scaffolds absorb water or physiological fluids through their internal pores, this can assist cells signaling and nutrition in scaffolds or provide route for the egress of drugs.[37] As represented in Figure 7, five scaffolds with varied PCL contents (8% PCL/4% PMMA/1% 6-MP), (4% PCL/4% PMMA/1% 6-MP),

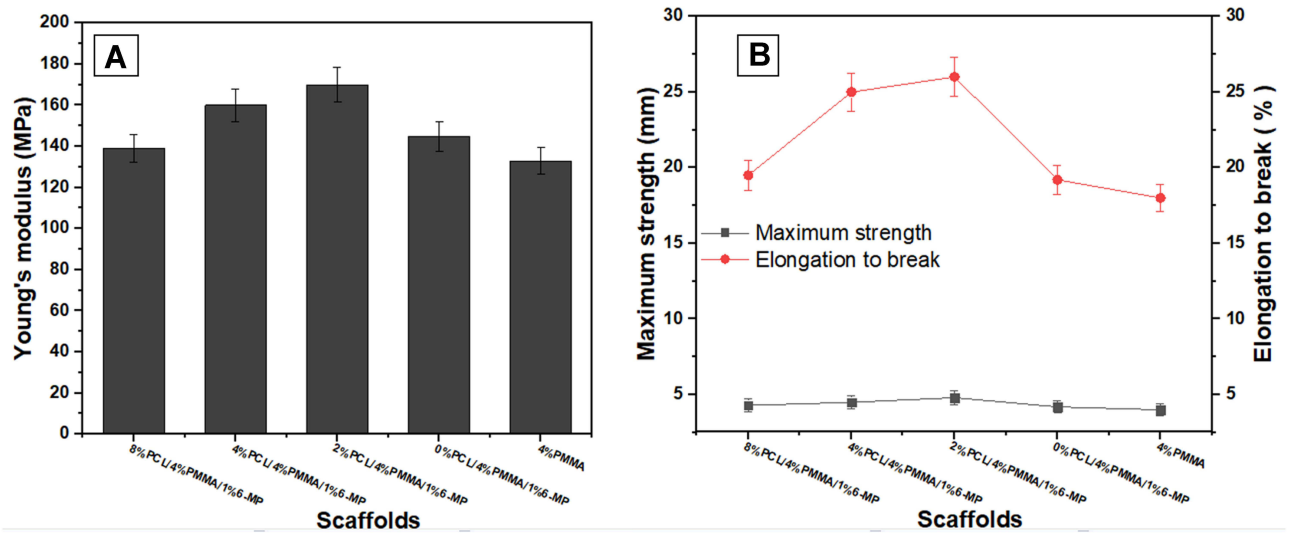

Figure 6 Mechanical properties, e.g., (**A**) Young's modulus, (**B**) maximum strength and elongation-to-break (%) of electrospun (8% PCL/4% PMMA/1% 6-MP), (4% PCL/4% PMMA/1% 6-MP), (2% PCL/4% PMMA/1% 6-MP), (4% PMMA/1% 6-MP) and 4% PMMA nanofiber scaffolds.

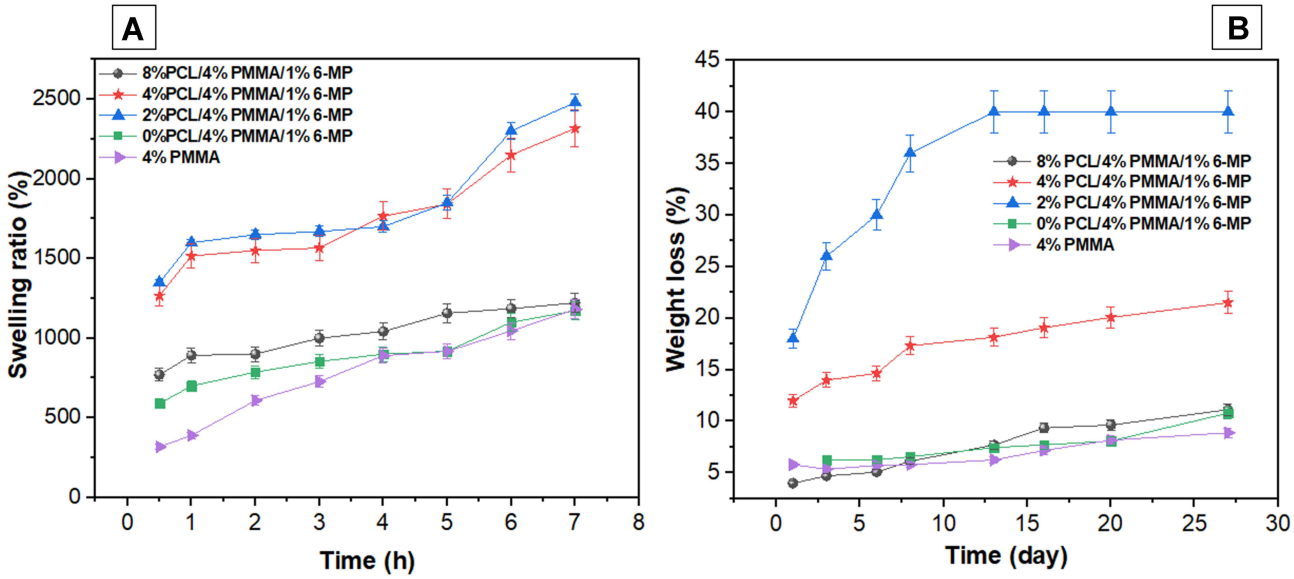

Figure 7 Physiochemical features of different nanofibrous mats (**A**) swelling ratio (%) and (**B**) weight loss (%).

(2% PCL/4% PMMA/1% 6-MP), (4% PMMA/1% 6-MP) and (4% PMMA) revealed different behavior when submerged in distilled water at pH 7.5, as a function of time. Swelling ratio of nanofibrous scaffolds was observed to be low and slowly due to the high hydrophobicity of PMMA/PCL polymers and drug, as well. Therefore, NFs mats exhibit low weight loss behavior in PBS; where (2% PCL/4% PMMA/1% 6-MP) exhibited the highest degree of degradation because it provided the highest swelling ratio, compared to unloaded-scaffold. This can be ascribed to the miscibility and amorphous structure of NFs mats as aforementioned proven by XRD analysis which thus allow more water molecules to diffuse through pores and swell the mats even further.

Antimicrobial Activities of Tested NFs Mats Against Multi-Drug Human Pathogens

There are different drug resistance profiles for human pathogens,[38] for example, the medical literature refers to different definitions for resistance; such as multidrug-resistant, extensively drug-resistant, in addition to pan

drug-resistant to describe the resistance of microbial pathogens against different antibiotics.[39] In this work, human pathogens were tested against different antibiotic categories; such as *Kanamycin* (30 mcg), *Ampicillin* (10 mcg) and *Cephaloridine* (30 µg) for bacterial cells; *Itraconazole* (10 µg), *Fluconazole* (25 mcg), and *Clotrimazole* (10 mcg) for fungal cells. Subsequently, "Extensively-Resistant" microbial cells were detected as those that resisted at least one of the tested antibiotics. Examples include *Klebsiella rhinoscleromatis, Streptococci sp*., and *Candida tropicalis*. On the other hand, *Klebsiella rhinoscleromatis* resisted to *Kanamycin* (30 mcg) but sensitive to both *Ampicillin* (10 mcg), and *Cephaloridine* (30 µg). But *Streptococci sp*., resisted *Ampicillin* (10 mcg) nevertheless sensitive to *Kanamycin* (30 mcg), and *Cephaloridine* (30 µg) discs. Additionally, *Candida tropicalis* was sensitive to both *Itraconazole* (10 µg), and *Fluconazole* (25 mcg) and resisted *Clotrimazole* (10 mcg). On the other hand, the "Pan drug-resistant" human pathogens were defined as non-susceptibility to all tested antibiotics NFs mats, (i.e., *Shigella sp., Staphylococcus epidermidis*, and *Candida krusei* (Table 3).

By comparing results of all fabricated electrospun 6-MP-loaded PMMA/PCL nanofibrous scaffolds, (2% PCL/4% PMMA/1% 6-MP) (C) recorded the highest inhibition zones against *Shigella spp*., (24.67±0.3) followed by *Candida krusei* (16.78±0.9), and *Staphylococcus epidermidis* (15.78±1.8). Also, (8% PCL/4% PMMA/1% 6-MP) (A), (4% PCL/4% PMMA/1% 6-MP) (B), and (1% 6-MP) (F), showed inhibition zones lower than (2% PCL/4% PMMA/1% 6-MP) NFs scaffolds (C). However, no inhibition zones were observed in case of (4% of PMMA) (E), as shown Figure 8. Generally, different concentrations of fabricated nanofibrous scaffolds inhibited the growth of different multi-drug-resistant human pathogens; which indicated that the antimicrobial efficacy exhibited due to existing 1% 6-MP. Since, mats that free of 1% 6-MP (E) showed no inhibition zones against all tested microbes. Also, there are many studies used biodegradable PCL-based films incorporated with PMMA and different drugs or nanoparticles which reported that these mats have no antimicrobial activities individually.[40–42]

Different mats compositions of electrospun PMMA/PCL/6-MP nanofibers coded as (A) (8% PCL/4% PMMA/1% 6-MP), (B) (4% PCL/4% PMMA/1% 6-MP), and (C) (2% PCL/4% PMMA/1% 6-MP) were tested against extensively drug-resistant human pathogens (*Klebsiella rhinoscleromatis, Streptococci sp*., and *Candida tropicalis*) as shown in Figure 9. We noticed that, the highest inhibition zones were found for NFs (2% PCL/4% PMMA/1% 6-MP) (C) against *Candida tropicalis* (39.43±3.5), and *Klebsiella rhinoscleromatis* (35.37 ±0.9) followed by *Streptococci sp*., (29.25±2.2). While, the lowest inhibition zones were recorded against *Klebsiella rhinoscleromatis* (20.83±2.0) followed by *Streptococci spp*, (22.33±1.3), and *Candida tropicalis* (23.63±0.1) in case of NFs of (8% PCL/4% PMMA/1% 6-MP) (A). Previously, different immunosuppressive and anti-inflammatory drugs, i.e., 6-MP, and azathioprine (AZA) were tested to inhibit the growth of gastrointestinal human pathogens significantly such as *campylobacter concisus, Bacteroides fragilis, Bacteroides*

Table 3 Represented Antibiotic Susceptibility Test Using Different Antibiotics Such as Kanamycin (30 Mcg), Ampicillin (10 Mcg) and Cephaloridine (30 µg) for Bacterial Cells Besides Itraconazole (10 µg), Fluconazole (25 Mcg), and Clotrimazole (10 Mcg) for Fungal Cells

Human Pathogens	Antibiotic Sensitivity Discs		
	K-30 mcg	AMP-10 mcg	CH-30 µg
Shigella spp	R	R	R
Klebsiella rhinoscleromatis	R	S	S
Staphylococcus epidermidis	R	R	R
Streptococci spp	S	R	S
	IT-10 µg	FLC –25 mcg	CC-10mcg
Candida krusei	R	R	R
Candida tropicalis	S	S	R

Notes: Consequently, the synthesized compositions coded as A, B, C, D, E, and F were surveyed firstly against pan drug-resistant human pathogens, i.e., *Shigella spp*. (-ve), *Staphylococcus epidermidis* (+ve), and *Candida krusei* (Figure 8).

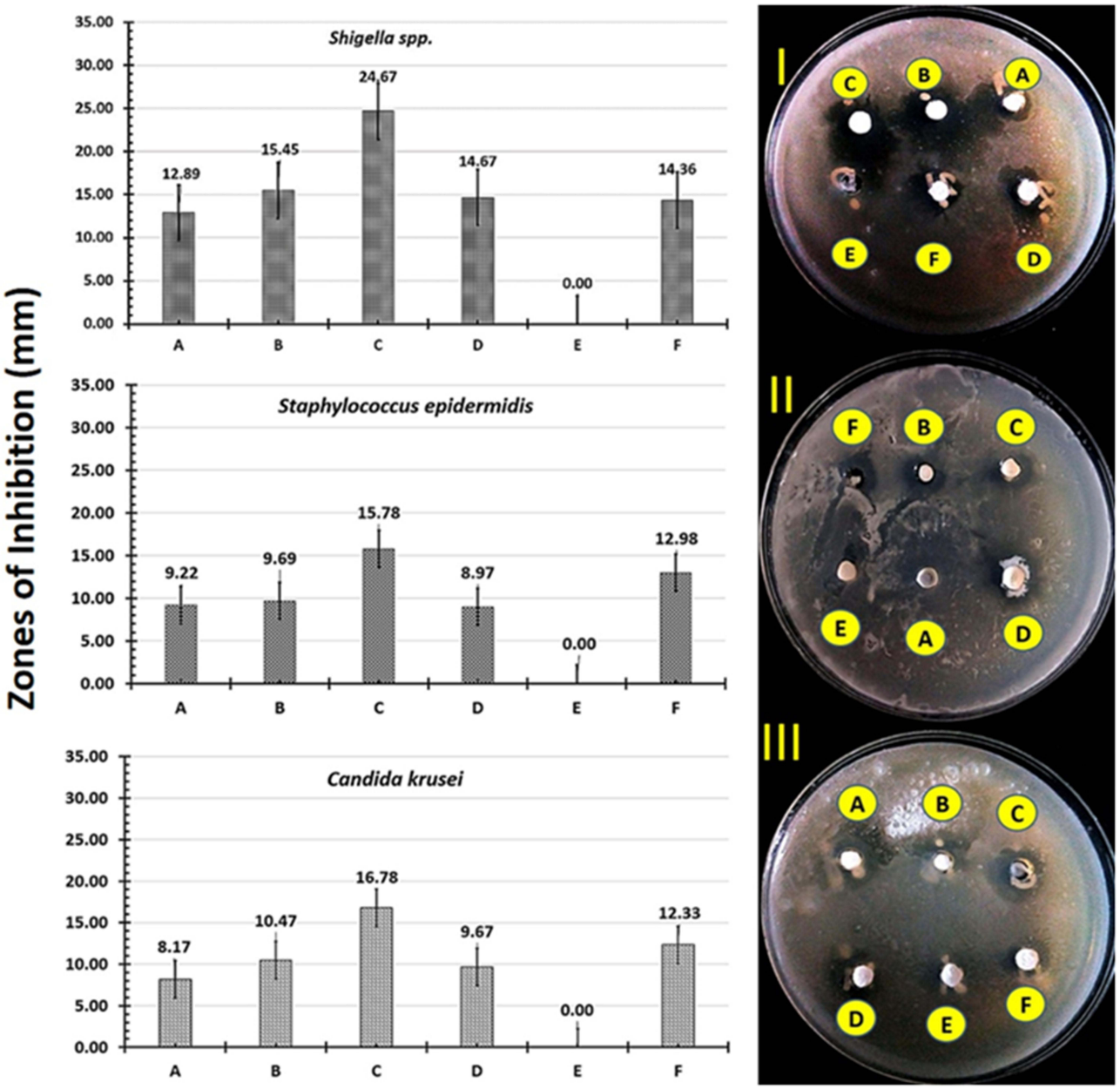

Figure 8 Antimicrobial activities of tested composite nanofibrous mats containing different concentrations of PCL: (8% PCL- 4% PMMA-1% 6-MP) (**A**), (4% PCL- 4% PMMA-1% 6-MP) (**B**), and (2% PCL-4% PMMA-1% 6-MP) (**C**), (4% PMMA-1% 6-MP) (**D**), (4% of PMMA) (**E**), and (1% 6-MP) (**F**) against *Shigella Spp.* (I), *Staphylococcus Epidermidis* (II), and *Candida Krusei* (III) using agar-well diffusion method.

vulgatus, and *E. coli*.[43] Lately, 6-MP has been reported as a significant antimicrobial agent against other human pathogens as mycobacterium avium.[44] Since, 6-MP was transformed to purine analogs that interfered with DNA synthesis depending on specific characters of human pathogens.[45,46]

Hemocompatibility Test of Nanofibrous Scaffolds

The hemolysis (%) test was applied to different NFs composites, where results of tests are summarized in Table 4. It was noticed that, the composition with high ratio of (PCL: PMMA) (2:1) showed the highest percentage of hemolysis, while the extent of hemolysis decreases for scaffolds composed of low ratios of (PCL: PMMA) as (1:1 and 1:2), respectively. The safety of an examined nanofibers towards RBCs obtained from a healthy individual could be presented and ordered according to the most hemo-compatible NFs as follows: (4%PCL/4%PMMA/1%6-MP) > (2%PCL/4% PMMA/1%6-MP) > (4%PMMA/1%6-MP) > (4%PMMA) > (8%PCL/4%PMMA /1%6-MP). These results might be attributed to the hydrophobic nature of PCL, PMMA and 6-MP which significantly favors protein-surface interaction

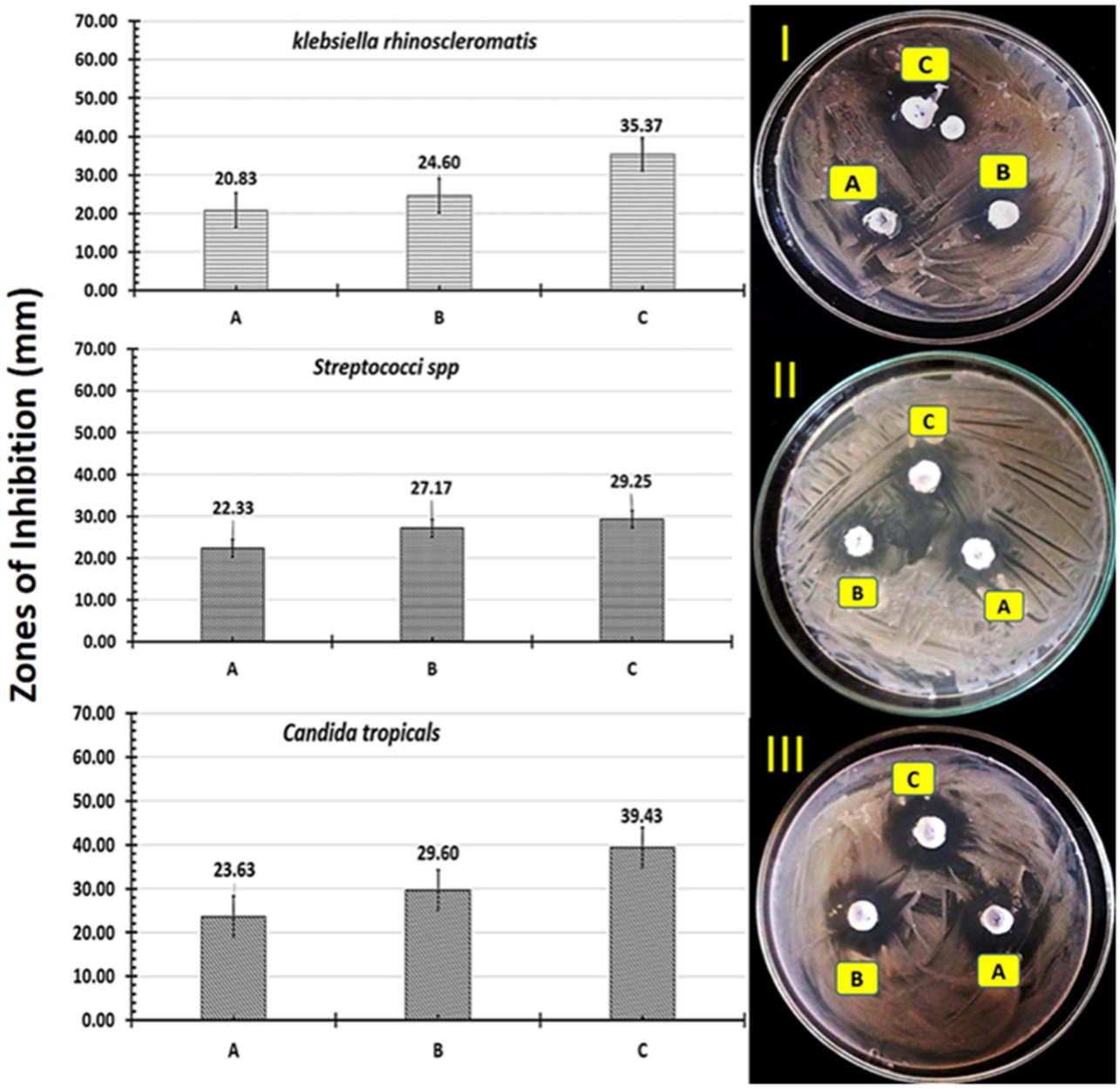

Figure 9 Antimicrobial activities of tested composite nanofibrous mats containing different concentrations of PCL: (8% PCL- 4% PMMA-1% 6-MP) (**A**), (4% PCL- 4% PMMA-1% 6-MP) (**B**), and (2%PCL- 4%PMMA-1% 6-MP) (**C**) against (*Klebsiella Rhinoscleromatis*, (I) *Streptococci Spp*. (II) and *Candida tropicalis* (III) using agar well diffusion method.

therefore enhanced thrombogenicity. These results were proven previously by Choubey et al,[47] who demonstrated the addition of high ratio of hydrophobic PCL to PMMA (2:1) which showed an increase in hemolysis (4.7%), compared to low ratios (1:1) and (1:2) which revealed decreasing in hemolysis to (2.3 and 2.6%), respectively.[47]

Drug Content Calculation

The mean 6-MP content and the loading efficiency in different NFs scaffolds were calculated and listed in Table 5 and Figure 10. All scaffolds showed high loading efficiency of 6-MP ranged from 90–97.5%, while the highest efficiency of 6-MP loading was scaffold which has the lowest PCL content, where the drug content was at 6.5%. These results established that the absence of drug loss during the electrospinning process and uniform distribution of the drug through 6-MP -loaded nanofiber scaffolds. This result is coupled with that achieved by El-Helaly et al,[48] who successfully loaded raloxifene onto different polymer nanofiber mats with efficiencies ranging from 92–103% dependent on the different composite ratio of NFs mats.

Table 4 Blood Hemolysis Assay (%) of Electrospun 6-MP Loaded-PMMA/PCL Nanofibrous Scaffolds Against Human Healthy Blood

Nanofiber Mats	Hemolysis (%)	
	1 mg/mL	2 mg/mL
(8%PCL/ 4%PMMA/ 1%6-MP)	68	87
(4%PCL/ 4%PMMA/ 1%6-MP)	2	5
(2%PCL/ 4%PMMA/ 1%6-MP)	3	10
(4%PMMA/ 1%6-MP)	43	71
(4%PMMA)	51	81
Positive control	100	100

In vitro Drug Release Profile from 6-MP-Loaded Nanofibrous Mats

Figure 11 shows 6-MP release behavior from different drug-loaded nanofibrous mats. Drug release rates are strongly depending on drug hydrophilicity and the incorporation method to the polymer matrix.[35] As shown in Figure 11, scaffold of (4%PMMA/1%6-MP) showed the lowest level of release of 6-MP in the buffer solution, due to the hydrophobicity of PMMA carrier scaffold in addition to the good dispersion and high miscibility between 6-MP and PMMA. However, scaffolds of (4%PCL/4%PMMA/1%6-MP) and (2%PCL/4%PMMA/1%6-MP) released 18 and 20% of 6-MP after 23 h, respectively and the release profile was kept pretty constant for more than 20 days. It is well known that, DMF as a good solvent for both PMMA and 6-MP resulted in high miscibility between 6-MP and high ratio of PMMA nanofibers resulting in stabilize of 6-MP in the core of scaffold. On the other hand, DCM as a typical solvent of PCL and a poor solvent for 6-MP, thus high ratio of PCL nanofibers resulted in 6-MP aggregating on the surface of scaffold and sudden burst release occurring with 60% at first 2 hours. The results ensured that, a sustained 6-MP release profile leading to targeted decrease its toxicity effect on the surrounded and contacted cells. Whilst, the drug release can be enhanced efficiently from the hydrophobic scaffold by enzymatic degradation as previously proven by Yuan et al.[35]

Cytotoxicity Test of Electrospun PCL/PMMA/6-MP Nanofibrous Scaffolds

Cell viability (%) of tested NFs mats was estimated by MTT assay using *HFB-4* cell line, as presented in Figure 12. The recorded results indicate that, all tested nanofibers promote proliferation of *HFB-4* in a concentration-dependent manner, related to control after 3 days of cell treatment. The observed viability of cells recorded at 98, 99, 96, 98 and 99.5% for G1, G2, G3, G4 and G5, respectively for exposure to lower concentration of NFs (0.125 mg/mL). The cell viability at higher concentration (2 mg/mL) was recorded to be 73, 55, 63, 65, 79%, respectively. Previously, it was found that the platform of PCL/PMMA was a safe on the cell and appropriate for cell proliferation.[34] However, 6-MP as chemotherapeutic agent have many undesirable properties but the most critical one is cytotoxicity toward the normal cells. Herein, the results demonstrated that all sandwiching 6-MP-loaded nanofibrous scaffolds were extensively safe on the normal cells even with using high concentrations of NFs. This result is consistent with those of Kushwaha et al,[2] who successfully loaded 6-MP onto hollow mesoporous silica nanoparticles to increase its release efficiency and reduce cytotoxicity of 6-MP.

Anticancer Activity of PCL/PMMA/6-MP Nanofibrous Scaffolds

The anticancer effect of different 6-MP-loaded mats with different PCL contents as (8%PCL/4%PMMA/1%6-MP), (4%PCL/4%PMMA/1%6-MP), (2%PCL/4%PMMA/1%6-MP), (4%PMMA/1%6-MP and 4%PMMA) were investigated on various cancerous cell lines, e.g., (*Caco-2, HepG-2* and *MDA* cell lines) which were specified for (colon cancer, liver cancer and breast cancer),

Table 5 Drug Content and Its Loading Efficiency on Different Nanofiber Scaffolds

Scaffold	Amount of Drug (mg)	Scaffold Weight (mg)	Drug Capacity (%)	Drug Loading Efficiency (%)
8%PCL/ 4%PMMA/ 1%6-MP	18	720	2.5	90
4%PCL/ 4%PMMA/ 1%6-MP	19.2	320	6	96
2%PCL/ 4%PMMA/ 1%6-MP	19.5	300	6.5	97.5
4%PMMA/ 1%6-MP	19	205	9.2	95

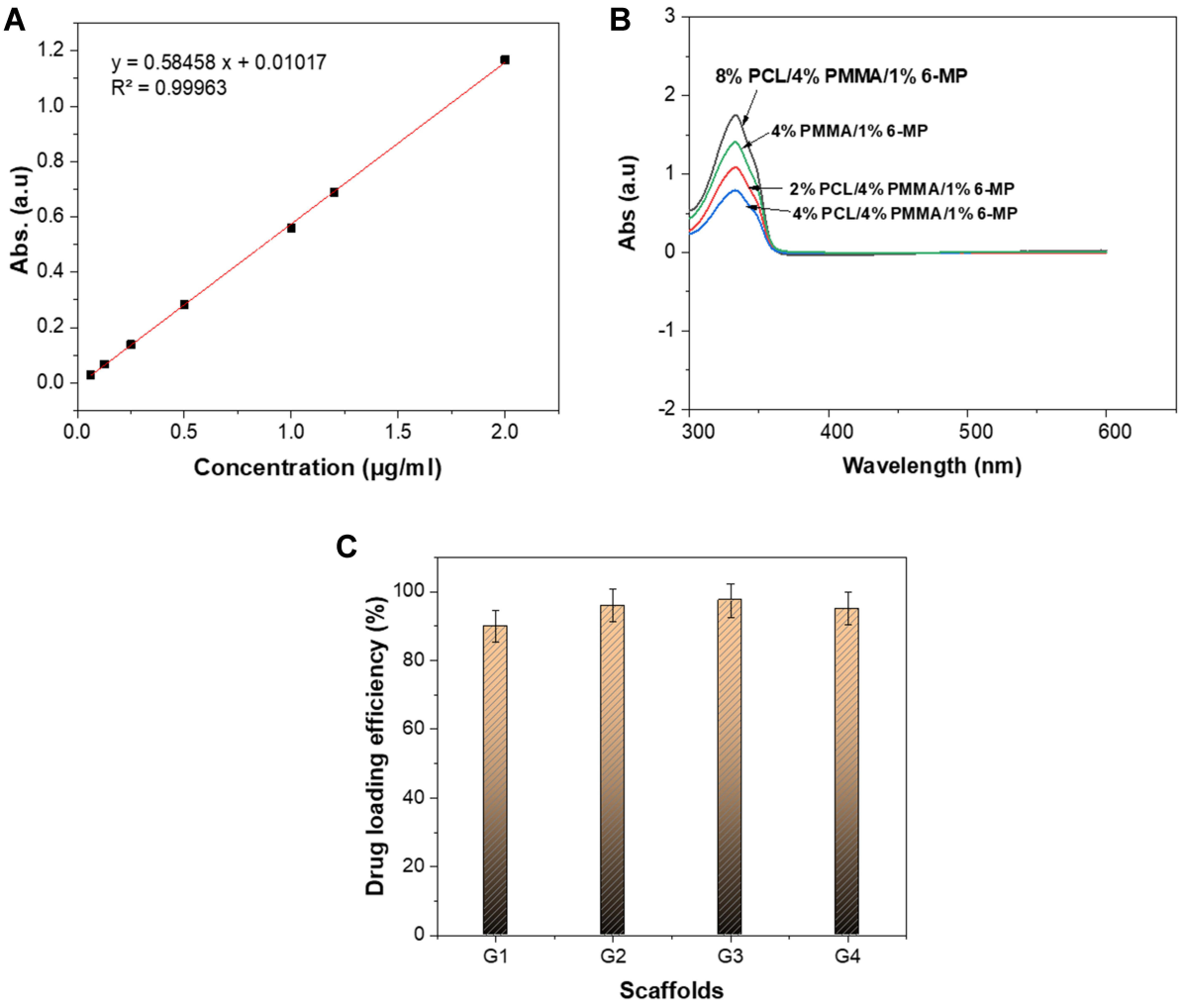

Figure 10 Assay of drug content (**A**) Calibration curve of 6-MP, (**B**) standard curve for drug content using UV spectroscopy and (**C**) drug-loading efficiency of different nanofiber scaffolds.

respectively. By using MTT assay, the viability of different cancerous cells was observed after three days of incubation with tested nanofibers, as shown in Figure 13. The results indicate that; all 6-MP-loaded sandwich scaffolds have a wide anticancer effect on different types of cancer cell lines. Both nanofibrous sandwich scaffolds composed of (4%PCL/4% PMMA/1%6-MP) and (2%PCL/4%PMMA/1%6-MP) demonstrated the lowest viability of all cancerous cell lines and this clarified by high miscibility and homogeneity between 6-MP and PCL/PMMA polymers. The sandwich tri-layered electrospun nanofiber mats revealed the successful model of sustained release of 6-MP which affected directly and obviously on cancer cell lines viability and kept a safe on the normal cell at the same concentration and environment.

As shown in Figure 13, when the cells were mixed with 2 mg/mL of (2%PCL/4%PMMA/1%6-MP) the cell viability of (*Caco-2, HepG-2* and *MDA* cells) dropped to almost 12%. However, the same concentration was less toxic for the normal cells, which have a viability around 66%. Likewise, the viability of different cancer cell lines was broken down to 18, 15 and 27% when treated with (4%PCL/4%PMMA/1%6-MP) nanofibrous mat. Additionally, sandwich 6-MP-loaded PMMA nanofibers represented reduction of the cancerous cell lines (*Caco-2, HepG-2* and *MDA* cells) to be recorded as 20, 25 and 29%, respectively; compared to control PMMA scaffold. The selectivity of nanofibrous scaffold to cancer cells is consider a critical factor for the treatment manner. From Table 6, it was concluded that IC_{50} values of (2%PCL/4%PMMA/1%6-MP) varied from 0.3 mg/mL for *MDA*

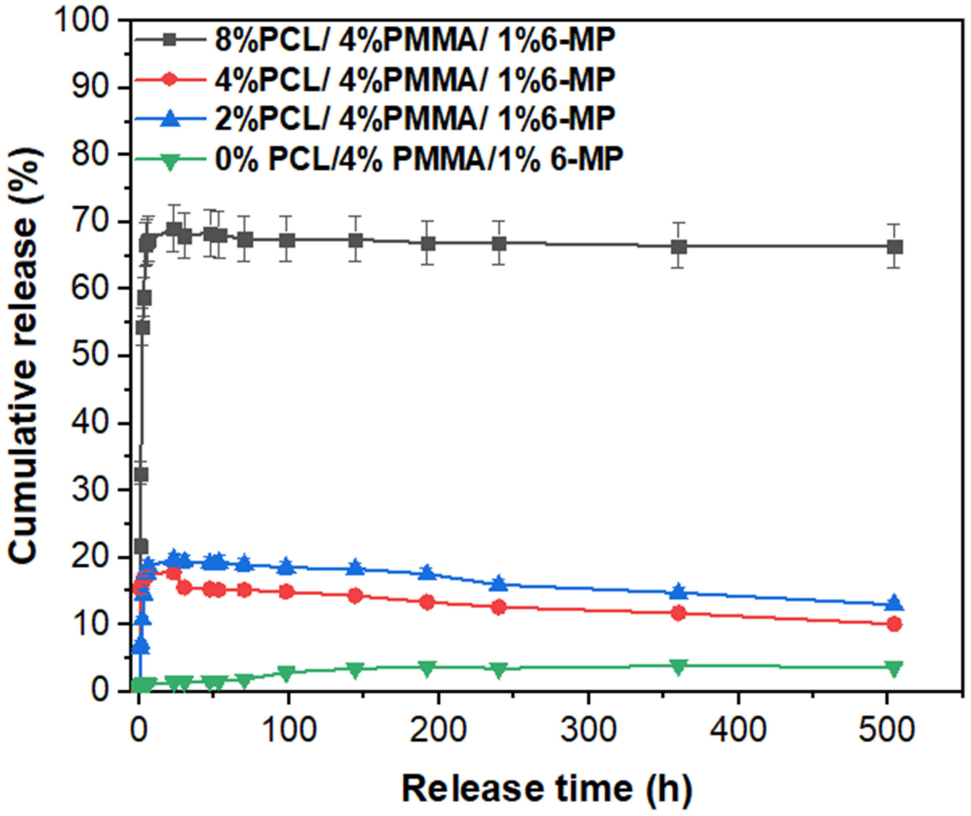

Figure 11 In vitro drug release profiles of 6-MP loaded PCL/PMMA nanofibrous mats.

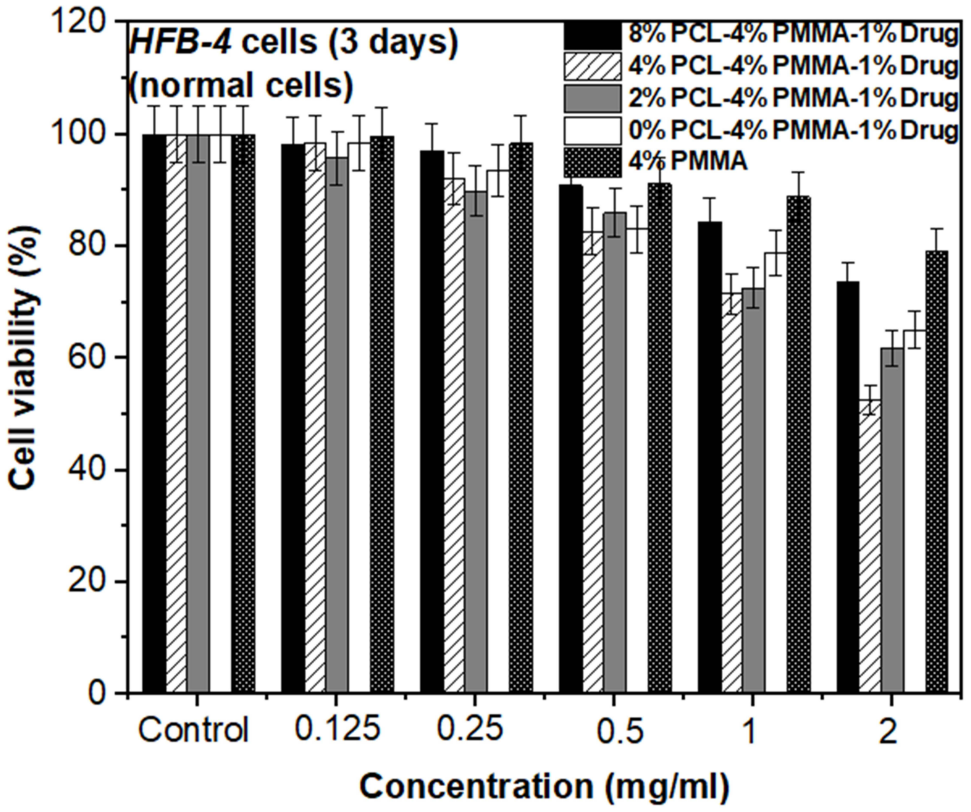

Figure 12 Cell viability (%) of different nanofibrous scaffolds (8%PCL/4%PMMA/1%6-MP), (4%PCL/4%PMMA/1%6-MP), (2%PCL/4%PMMA/1%6-MP), (4%PMMA/1%6-MP) and 4% PMMA.

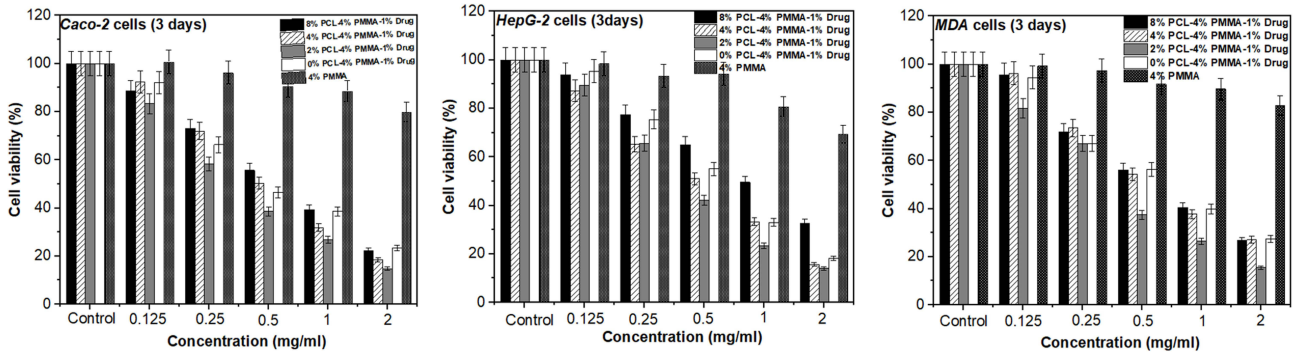

Figure 13 Anticancer assay of different 6-MP loaded- PCL/PMMA nanofiber mats treated with various cancer cell lines as *Caco-2*, *MDA* and *HepG-2* cells.

cells (breast cancer) to 3.3 mg/mL for *HFB-4* cells (normal cell). Meanwhile, Table 7, concluded that the high ratio of PMMA enhanced the selective index of the different cancer cells specifically breast cancer cells.

Conclusion

The sandwich configurations of 6-MP-loaded PMMA/PCL nanofibrous mats were made-up by electrospinning technique and extensively evaluated for their efficiency in controlled manner of drug release. It was evident that (4% PCL/4%PMMA/1%6-MP), (2%PCL/4%PMMA/1%6-MP) and (4%PMMA/1%6-MP) revealed minimal initial burst and controlled drug release for 21 days than (8% PCL/4% PMMA/1%6-MP). Moreover, XRD results established that hydrophobic drug of 6-MP was amorphized during fabrication process which ultimately improved the dissolution properties. Further, the crystallinity (%) of the sandwich scaffolds imparted by the flanking layers of PMMA/PCL modulated 6-MP release. The outcomes of this study suggest that, the ratio of PCL to PMMA in the flanking layers is strongly affected the initial burst and long-term release of 6-MP release profile. The anti-microbial properties of mats

Table 6 IC_{50} (95% Confidence Intervals) of Electrospun 6-MP Loaded-PCL/PMMA Nanofibrous Scaffolds

Composition of Nanofiber Mats	IC_{50} (95% Confidence Intervals) (mg/mL) Using Different Cancer Cell-Lines			
	HFB-4 Cells	*Caco-2* Cells	*MDA* Cells	*HepG-2* Cells
(8%PCL/4%PMMA/1%6-MP)	5.414 (3.934: 7.450)	0.6476 (0.5718: 0.7333)	0.7009 (0.4747: 1.035)	0.9641 (0.7572: 1.228)
(4%PCL/4%PMMA/1%6-MP)	2.188 (1.843: 2.598)	0.5497 (0.4393: 0.6879)	0.6766 (0.4491: 1.019)	0.5077 (0.4071: 0.6332)
(2%PCL/4%PMMA/1%6-MP)	3.306 (2.399: 4.554)	0.376 (0.2845: 0.4969)	0.3555 (0.2591: 0.4878)	0.4244 (0.3404: 0.5291)
(4%PMMA/1%6-MP)	3.928 (2.111: 7.312)	0.5626 (0.3474: 0.9112)	0.6767 (0.4223: 1.084)	0.6056 (0.4944: 0.7418)
(4%PMMA)	7.545 (2.871: 19.83)	9.429 (2.471: 35.98)	13.13 (3.954: 43.57)	4.135 (2.282: 7.495)

Table 7 Selective Index (SI) of Electrospun 6-MP-Loaded PCL/PMMA Nanofibrous Scaffolds

Composition of Nanofiber Mats	Selective Index (SI)		
	Caco-2 Cells	*MDA* Cells	*HepG-2* Cells
(8% PCL/4% PMMA/1% 6-MP)	3.2	4.5	2.7
(4% PCL/4% PMMA/1% 6-MP)	4.5	5	3.6
(2% PCL/4% PMMA/1% 6-MP)	5.1	5.6	4.3
(4% PMMA/1% 6-MP)	4.3	3.5	2.7
(4% PMMA)	1.5	1.6	1.5

were studied against different bacterial and fungal strains (*Shigella sp., Klebsiella rhinoscleromatis, Staphylococcus epidermidis, Streptococci sp., Candida krusei and Candida tropicalis*) to reveal the clear inhibition zone surrounded all 6-MP-loaded-tri-layered scaffolds. Moreover, these nanofibrous scaffolds were investigated for cytotoxicity with *HFB-4* cell line and were established to be nontoxic. Moreover, the anti-cancer activity showed that the viability of cancerous cells (*Caco-2, HepG-2* and *MDA* cells) decreased to almost 12% when cells mixed with 2 mg/mL of (2%PCL/4%PMMA/1%6-MP). Accordingly, we reinstate our hypothesis that sandwiching 6-MP-loaded electrospun tri-layered scaffolds of lipophilic PMMA/PCL effectively enhance sustained drug release. To summarize, (2%PCL/4%PMMA/1%6-MP) and (4%PCL/4%PMMA / 1%6-MP) sandwich scaffolds with comparatively desired drug release profile amongst other groups in the study need to be further examined in vivo for assessing its potential in cancer treatment.

Acknowledgments

Special thanks are extended to Prof. Dr. Samah A. Loutfy, Virology and Immunology Unit, Cancer Biology Department, National Cancer Institute, Cairo University, Egypt for donating 6-MP drug.

Funding

There was no fund established for conducting this work.

Disclosure

The authors report no conflicts of interest in this work.

References

1. Roberts C, Strauss VY, Kopijasz S, et al. Results of a phase II clinical trial of 6-mercaptopurine (6MP) and methotrexate in patients with BRCA-defective tumours. *Br J Cancer*. 2020;122(4):483–490. doi:10.1038/s41416-019-0674-4
2. Kushwaha SKS, Rai AK. 6-mercaptopurine loaded mesoporous silica nanoparticles as sustained drug delivery for cancer. *Bionanoscience*. 2020;10:672–682. doi:10.1007/s12668-020-00751-z
3. Ahmed AH, Badr YAE. Improvement of 6-mercaptopurine efficiency by encapsulated in chitosan nanoparticles. *Arab J Nucl Sci Appl*. 2018;51(4):181–186.
4. Cuin A, Massabni AC, Pereira GA, et al. 6-mercaptopurine complexes with silver and gold ions: anti-tuberculosis and anti-cancer activities. *Biomed Pharmacother*. 2011;65(5):334–338. doi:10.1016/j.biopha.2011.04.012
5. Kevadiya BD, Chettiar SS, Rajkumar S, Bajaj HC, Gosai KA, Brahmbhatt H. Evaluation of Clay/Poly (L-Lactide) microcomposites as anticancer drug, 6-mercaptopurine reservoir through in vitro cytotoxicity, oxidative stress markers and in vivo pharmacokinetics. *Colloids Surf B Biointerf*. 2013;112:400–407. doi:10.1016/j.colsurfb.2013.07.008
6. Panetta JC, Evans WE, Cheok MH. Mechanistic mathematical modelling of mercaptopurine effects on cell cycle of human acute lymphoblastic leukaemia cells. *Br J Cancer*. 2006;94(1):93–100. doi:10.1038/sj.bjc.6602893
7. Cheok MH, Evans WE. Acute lymphoblastic leukaemia: a model for the pharmacogenomics of cancer therapy. *Nat Rev Cancer*. 2006;6(2):117–129. doi:10.1038/nrc1800
8. Grossen P, Witzigmann D, Sieber S, Huwyler J. PEG-PCL-based nanomedicines: a biodegradable drug delivery system and its application. *J Control Release*. 2017;260:46–60. doi:10.1016/j.jconrel.2017.05.028
9. Pina S, Ribeiro VP, Marques CF, et al. Scaffolding strategies for tissue engineering and regenerative medicine applications. *Materials (Basel)*. 2019;12(11):1824. doi:10.3390/ma12111824
10. Gamez E, Mendoza G, Salido S, Arruebo M, Irusta S. Antimicrobial electrospun polycaprolactone-based wound dressings: an in vitro study about the importance of the direct contact to elicit bactericidal activity. *Adv Wound Care*. 2019;8(9):438–451. doi:10.1089/wound.2018.0893
11. Malikmammadov E, Tanir TE, Kiziltay A, Hasirci V, Hasirci N. PCL and PCL-based materials in biomedical applications. *J Biomater Sci Polym Ed*. 2018;29(7–9):863–893. doi:10.1080/09205063.2017.1394711
12. Hernandez JL, Park J, Yao S, et al. Effect of tissue microenvironment on fibrous capsule formation to biomaterial-coated implants. *Biomaterials*. 2021;273:120806. doi:10.1016/j.biomaterials.2021.120806
13. Sivakumar M, Subadevi R, Rajendran S, Wu H-C, Wu N-L. Compositional effect of PVdF–PEMA blend gel polymer electrolytes for lithium polymer batteries. *Eur Polym J*. 2007;43(10):4466–4473. doi:10.1016/j.eurpolymj.2007.08.001
14. Subban RHY, Arof AK. Plasticiser interactions with polymer and salt in PVC–LiCF3SO3–DMF electrolytes. *Eur Polym J*. 2004;40(8):1841–1847. doi:10.1016/j.eurpolymj.2004.03.026
15. Stephan AM, Kumar TP, Renganathan NG, Pitchumani S, Thirunakaran R, Muniyandi N. Ionic conductivity and FT-IR studies on plasticized PVC/PMMA blend polymer electrolytes. *J Power Sources*. 2000;89(1):80–87. doi:10.1016/S0378-7753(00)00379-7
16. Chen T, Kusy RP. Effect of methacrylic acid: methyl methacrylate monomer ratios on polymerization rates and properties of polymethyl methacrylates. *J Biomed Mater Res*. 1997;36(2):190–199. doi:10.1002/(SICI)1097-4636(199708)36:2<190::AID-JBM7>3.0.CO;2-F
17. Preshaw PM, Walls AWG, Jakubovics NS, Moynihan PJ, Jepson NJA, Loewy Z. Association of removable partial denture use with oral and systemic health. *J Dent*. 2011;39(11):711–719. doi:10.1016/j.jdent.2011.08.018
18. Abdelrazek EM, Hezma AM, El-Khodary A, Elzayat AM. Spectroscopic studies and thermal properties of PCL/PMMA biopolymer blend. *Egypt J Basic Appl Sci*. 2016;3(1):10–15.
19. Ma K, Qiu Y, Fu Y, Ni -Q-Q. Electrospun sandwich configuration nanofibers as transparent membranes for skin care drug delivery systems. *J Mater Sci*. 2018;53(15):10617–10626. doi:10.1007/s10853-018-2241-4
20. Yang Y, Chang S, Bai Y, Du Y, Yu D-G. Electrospun triaxial nanofibers with middle blank cellulose acetate layers for accurate dual-stage drug release. *Carbohydr Polym*. 2020;243:116477. doi:10.1016/j.carbpol.2020.116477
21. Cai L, Shi H, Cao A, Jia J. Characterization of gelatin/chitosan polymer films integrated with docosahexaenoic acids fabricated by different methods. *Sci Rep*. 2019;9(1):1–11. doi:10.1038/s41598-019-44807-x
22. Chen DW-C, Liao J-Y, Liu S-J, Chan E-C. Novel biodegradable sandwich-structured nanofibrous drug-eluting membranes for repair of infected wounds: an in vitro and in vivo study. *Int J Nanomedicine*. 2012;7:763.

23. Wang M, Hou J, Yu D-G, Li S, Zhu J, Chen Z. Electrospun tri-layer nanodepots for sustained release of acyclovir. *J Alloys Compd*. 2020;846:156471. doi:10.1016/j.jallcom.2020.156471
24. Kamath SM, Sridhar K, Jaison D, et al. Fabrication of tri-layered electrospun polycaprolactone mats with improved sustained drug release profile. *Sci Rep*. 2020;10(1):1–13. doi:10.1038/s41598-020-74885-1
25. Simões MCR, Cragg SM, Barbu E, De Sousa FB. The potential of electrospun poly (methyl methacrylate)/polycaprolactone core–sheath fibers for drug delivery applications. *J Mater Sci*. 2019;54 (7):5712–5725. doi:10.1007/s10853-018-03261-2
26. Elsayed RE, Madkour TM, Azzam RA. Tailored-design of electrospun nanofiber cellulose acetate/poly (lactic acid) dressing mats loaded with a newly synthesized sulfonamide analog exhibiting superior wound healing. *Int J Biol Macromol*. 2020;164:1984–1999. doi:10.1016/j.ijbiomac.2020.07.316
27. Witherell KS, Price J, Bandaranayake AD, Olson J, Call DR. In vitro activity of antimicrobial peptide CDP-B11 alone and in combination with colistin against colistin-resistant and multidrug-resistant Escherichia coli. *Sci Rep*. 2021;11(1):1–10. doi:10.1038/s41598-021-81140-8
28. Moghnieh R, Araj GF, Awad L, et al. A compilation of antimicrobial susceptibility data from a network of 13 Lebanese hospitals reflecting the national situation during 2015–2016. *Antimicrob Resist Infect Control*. 2019;8(1):1–17. doi:10.1186/s13756-019-0487-5
29. Wayne PA. Clinical and laboratory standards institute: performance standards for antimicrobial susceptibility testing: 20th informational supplement. CLSI Doc. M100-S20; 2010.
30. Nasef SM, Khozemy EE, Kamoun EA, El-Gendi H. Gamma radiation-induced crosslinked composite membranes based on polyvinyl alcohol/chitosan/AgNO3/vitamin E for biomedical applications. *Int J Biol Macromol*. 2019;137:878–885. doi:10.1016/j.ijbiomac.2019.07.033
31. Mosmann T. Rapid colorimetric assay for cellular growth and survival: application to proliferation and cytotoxicity assays. *J Immunol Methods*. 1983;65(1–2):55–63. doi:10.1016/0022-1759(83)90303-4
32. Almahdy O, El-Fakharany EM, Ehab E-D, Ng TB, Redwan EM. Examination of the activity of camel milk casein against hepatitis C virus (Genotype-4a) and its apoptotic potential in hepatoma and hela cell lines. *Hepat Mon*. 2011;11(9):724. doi:10.5812/kowsar.1735143X.1367
33. Salim SA, Loutfy SA, El-Fakharany EM, Taha TH, Hussien Y, Kamoun EA. Influence of chitosan and hydroxyapatite incorporation on properties of electrospun PVA/HA nanofibrous mats for bone tissue regeneration: nanofibers optimization and in-vitro assessment. *J Drug Deliv Sci Technol*. 2021;62:102417. doi:10.1016/j.jddst.2021.102417
34. Son S-R, Linh N-TB, Yang H-M, Lee B-T. In vitro and in vivo evaluation of electrospun PCL/PMMA fibrous scaffolds for bone regeneration. *Sci Technol Adv Mater*. 2013;14:015009. doi:10.1088/1468-6996/14/1/015009
35. Yuan Y, Choi K, Choi S-O, Kim J. Early stage release control of an anticancer drug by drug-polymer miscibility in a hydrophobic fiber-based drug delivery system. *RSC Adv*. 2018;8 (35):19791–19803. doi:10.1039/C8RA01467A
36. Elashmawi IS, Hakeem NA. Effect of PMMA addition on characterization and morphology of PVDF. *Polym Eng Sci*. 2008;48 (5):895–901. doi:10.1002/pen.21032
37. Croisier F, Jérôme C. Chitosan-based biomaterials for tissue engineering. *Eur Polym J*. 2013;49(4):780–792. doi:10.1016/j.eurpolymj.2012.12.009
38. Lei J, Sun L, Huang S, et al. The antimicrobial peptides and their potential clinical applications. *Am J Transl Res*. 2019;11(7):3919.
39. Weinstein MP, Lewis JS, Kraft CS. The clinical and laboratory standards institute subcommittee on antimicrobial susceptibility testing: background, organization, functions, and processes. *J Clin Microbiol*. 2020;58(3):e01864–19. doi:10.1128/JCM.01864-19
40. Dutta D, Goswami S, Dubey R, Dwivedi SK, Puzari A. Antimicrobial activity of silver-coated hollow poly (methylmethacrylate) microspheres for water decontamination. *Environ Sci Eur*. 2021;33(1):1–17. doi:10.1186/s12302-021-00463-5
41. Lyu JS, Lee J-S, Han J. Development of a biodegradable polycaprolactone film incorporated with an antimicrobial agent via an extrusion process. *Sci Rep*. 2019;9(1):1–11. doi:10.1038/s41598-019-56757-5
42. Sodagar A, Khalil S, Kassaee MZ, Shahroudi AS, Pourakbari B, Bahador A. Antimicrobial properties of poly (methyl methacrylate) acrylic resins incorporated with silicon dioxide and titanium dioxide nanoparticles on cariogenic bacteria. *J Orthod Sci*. 2016;5(1):7. doi:10.4103/2278-0203.176652
43. Liu F, Ma R, Riordan SM, et al. Azathioprine, mercaptopurine, and 5-aminosalicylic acid affect the growth of IBD-associated campylobacter species and other enteric microbes. *Front Microbiol*. 2017;8:527.
44. Shin SJ, Collins MT. Thiopurine drugs azathioprine and 6-mercaptopurine inhibit mycobacterium paratuberculosis growth in vitro. *Antimicrob Agents Chemother*. 2008;52(2):418–426. doi:10.1128/AAC.00678-07
45. Greenstein RJ, Su L, Haroutunian V, Shahidi A, Brown ST. On the action of methotrexate and 6-mercaptopurine on M. Avium subspecies paratuberculosis. *PLoS One*. 2007;2(1):e161. doi:10.1371/journal.pone.0000161
46. Sieswerda LE, Bannatyne RM. Mapping the effects of genetic susceptibility and mycobacterium avium subsp. Paratuberculosis infection on Crohn's disease: strong but independent. *J Clin Microbiol*. 2006;44(3):1204–1205. doi:10.1128/JCM.44.3.1204-1205.2006
47. Choubey R, Chouhan R, Bajpai AK, Bajpai J, Singh SK. Silver hydroxyapatite (AgHAP) reinforced nanocomposites of poly (methyl methacrylate)-poly (ε-caprolactone) as hybrid orthopedic materials. *Int J Polym Mater Polym Biomater*. 2021;70(11):782–796. doi:10.1080/00914037.2020.1765353
48. Nageeb El-Helaly S, Abd-Elrasheed E, Salim SA, Fahmy RH, Salah S, El-Ashmoony MM. Green nanotechnology in the formulation of a novel solid dispersed multilayered core-sheath raloxifene-loaded nanofibrous buccal film; in vitro and in vivo characterization. *Pharmaceutics*. 2021;13(4):474. doi:10.3390/pharmaceutics13040474